NMR study of Li adsorbed on the Si(111)-(3×1)-Li surface

C. Bromberger, H. J. Jänsch, O. Kühlert, R. Schillinger, and D. Fick
Philipps-Universität, Fachbereich Physik and Zentrum für Materialwissenschaften, D-35032 Marburg, Germany
(Received 2 December 2003; revised manuscript received 27 February 2004; published 30 June 2004)

Li adsorption on the (3×1)-Li reconstructed Si(111) surface has been studied by β-nuclear magnetic resonance experiments (measurements of T_1 times). A rich variety of temperature, coverage, and magnetic field dependencies were observed, which reflect a metal-semiconductor-metal transition while adsorbing Li with increasing coverage on a (7×7)-reconstructed Si(111) surface in such a way that the (3×1) reconstruction is driven. With the aid of a formulated concept of Li donors localized on a semiconducting surface the temperature dependence of relaxation rates for Li adsorbed at extremely low coverages (up to 0.01 ML) could be understood consistently. The donor energy of adsorbed Li on the (3×1) surface has been determined to be $E_D\approx100$ meV. This success proves additionally that the theoretical results of a completely ionized Li chain in the (3×1) reconstruction are correct. The observed semiconductor-metal transition for adsorption of 0.14 ML additional Li on the already (3×1)-reconstructed surface points to the existence of an empty state near the Fermi energy (probably the so-called S_1^- state). The diffusion energy of Li on the Si(111)-(3×1) surface could be estimated to be $E_{\mathrm{diff}}\approx410$ meV.

DOI: 10.1103/PhysRevB.69.245424 PACS number(s): 73.20.Hb, 76.60.−k, 68.43.Jk

I. INTRODUCTION

Due to its dangling bonds the Si(111) surface undergoes various types of reconstructions. Except for the Si(111)-(7×7) one, which has many hallmarks of a metallic surface, all the adsorbate driven ones stay semiconducting as the hydrogen terminated Si(111)-(1×1):H one or the metal adsorption driven Si(111)-(3×1) reconstructions (see Refs. 1–3 and references therein). Only the hydrogen terminated reconstruction preserves the small (1×1) unit cell of the Si(111) surface and is free of electronic surface states within the fundamental band gap. In contrast, a narrow almost dispersionless surface state pins the Fermi level of the (7×7) reconstructed surface thus causing its metallicity.[4–6] There are now also growing experimental and particularly theoretical indications for the importance of electron-electron correlations in understanding the electronic properties of the (7×7)-reconstructed surface and of the hydrogen terminated one.[7–9] As the metal driven (3×1) reconstructions are concerned with the importance of electron-electron correlations is less obvious despite the fact that they exhibit quite unusual surface chemical and electronic properties (low oxygen uptake and a large band gap, respectively) due to their quasi-one-dimensional structure.[10,11] Moreover the observation of an almost dispersionless surface state in photoemission experiments[3,12] also points to the importance of electron-electron correlations for this reconstruction, as it is underbound by 0.31 eV compared to local density approximation calculations.[13]

Since its first observation[14,15] the (3×1) reconstruction of the Si(111) surface has generated widespread interest. The semiconducting (3×1) structures can be formed by alkali metals, alkaline earths, and by Ag (Refs. 3 and 13–26) in a rather simple procedure (see Ref. 16 and references therein). Despite some uncertainties about the details of the atomic arrangement there is a consensus that this reconstruction is driven by the metal adsorbate and that the reconstruction is completed for monovalent adsorbates at a metal coverage of 1/3 of a monolayer (ML), measured in units of one Si(111) layer (see Refs. 13,16,18,22,23 and references therein). In all structural models[13,18–21,27] the metal atoms form one chain per unit cell. They are separated by Si chains. Among the proposed structural models, the recent "560560" model[19,20] and the similar honeycomb-chain-channel (HCC) model[13] have the lowest total energy and explain most of the structural features seen in scanning tunneling microscopy (STM) and diffraction experiments.

From energy considerations it seems obvious that the alkali metal atoms act as electron donors, saturating the unpaired Si dangling bond in the (3×1) reconstruction. This aside, very little is known about the role of the metal atom in the reconstruction itself. Albeit performed at elevated temperatures, recent nuclear magnetic resonance (NMR) experiments contributed information about the local geometry and the electronic structure of the Li site.[24] A large, positive electric field gradient at the adsorbed Li nucleus places the Li site inside surrounding Si atoms and not above the surface, in accordance with the "560560" and HCC models (see Fig. 1 in Ref. 19 for the "560560" model and Fig. 1 in Ref. 13 for the HCC model). Since it is known that for semiconductor surfaces experiments at as low temperatures as possible improve the spectroscopic quality of the data[1] it seemed important to us to resume the NMR experiments at as low sample temperatures as feasible and to extend them to the measurements of T_1 times.[28–30] They are a useful tool to study local density of states at the adsorbate. Such experiments have been feasible for Li adsorbates for some time.[31–33] "Local" really means here electron density at the adsorbed Li nucleus.

Even though the (3×1) reconstruction can be obtained by adsorption of various metal atoms the Li-induced reconstruction is of special interest because of the simple electronic structure of Li and its accessibility to NMR measurements. The favored models (HCC and "560560") have five Si sur-

face orbitals per unit cell and thus five surface states. There are altogether six electrons available to fill these states, five from the Si atoms and one from the Li atom. Since the surface is semiconducting three filled surface states and two empty ones are expected. The band structure calculated with the HCC model[13] confirms this reasoning; two occupied surface state bands (S_1^+, S_2^+) with positive inversion symmetry in respect to a mirror plane on the surface and one with a negative one (S_2^-) are found. The assignment of an inversion symmetry is based on the theoretical finding that the Li atoms, which drive the reconstruction, are fully ionized. Since T_1 times reflect among others local electronic properties they might be a useful tool to check this result.

Almost nothing is known yet about the local geometry, the electronic structure and spectroscopic properties of alkali-metal adsorbates on the (3×1)-reconstructed surface. This is not only an academic problem, since an easy way to produce a three domain Li-induced (3×1)-reconstructed Si(111) surface is Li adsorption of 1–2 ML and subsequent thermal desorption of the excess amount to induce the (3×1) structure.[16] This preparation relies entirely on thermal programmed desorption (TPD) spectroscopy and produces the desired structure reproducibly with minimum effort. But in doing so small quantities of adsorbed Li up to a few percent of a monolayer (ML) may be left, acting as a dopant of the surface.

II. EXPERIMENT

The experiments were conducted at the Max-Planck-Institute for Nuclear Physics in Heidelberg. The ^{8}Li-β-NMR technique has already been described elsewhere in detail.[32,34,35] Therefore we describe this part of the experiment only briefly.

The experiments were performed in an UHV chamber with a base pressure of about 5×10^{-11} mbar. The chamber was equipped with conventional surface characterization techniques such as low-energy electron diffraction (LEED), Auger electron spectroscopy (AES) and a mass spectrometer for temperature programmed desorption (TPD) measurements. A Li getter source (SAES Getters) was also available. The chamber was equipped with a homemade load lock for a fast transfer of the silicon crystals.

The samples used were modestly p(B)- and n(P)-doped Si(111) crystals with a misorientation of $<0.5°$. They were prepared outside the UHV chamber as hydrogen terminated Si(111)-(1×1):H surfaces with a wet chemical procedure.[33,36] This detour was chosen in order to deal outside the UHV chamber with rather inert surfaces, which moreover are improved in their properties during the wet chemical treatment.[33] The as prepared samples were transferred into the UHV chamber via the fast load lock and clamped onto a small Mo plate on the vertically mounted manipulator. Heating was available by electron bombardment from the rear, cooling by contact to a liquid nitrogen reservoir. After the sample was transferred into the UHV it was flashed to about 1200 K in order to remove the adsorbed hydrogen and to enforce the (7×7) reconstruction. Afterwards a clear (7×7) LEED pattern was observed. The cleanliness of the surface was monitored by AES. To achieve (3×1) reconstructions the samples were covered by about 2 ML of Li and heated up to about 850 K afterwards (see Ref. 16). At this temperature the surplus Li desorbs and the mobility of the surface atoms is high enough to form the (3×1) reconstruction as also observed by LEED (see Ref. 10). The Li coverages θ_{Li} of the individual (3×1) reconstructions were determined by integrals over TPD spectra (see Ref. 37).

At coverages below 0.29 ML the Si(111) surface is only partially (3×1) reconstructed while the remaining surface is still (7×7) reconstructed. STM experiments showed that the (3×1) reconstruction nucleates at step edges.[17,38] And indeed, in the present experiments LEED patterns displayed both (7×7) and (3×1) ones at the same time. A full reconstructed (3×1) surface was observed in LEED already for coverages of $\theta_{\mathrm{Li}}=0.29\pm0.02$ ML. This is in quite good accordance with the results of Ref. 16 and with the structural models ("560560"[19] and HCC[13]) which contain only one Li Atom per (3×1) unit cell and thus a coverage of $\theta_{\mathrm{Li}}=1/3$ ML. The fact that already at a coverage of $\theta_{\mathrm{Li}}=0.29\pm0.02$ ML a full reconstructed (3×1) surface is observed in LEED can be understood either by the error in the coverage calibration by TPD (about ±0.02 ML), or by the fact that at about this coverage there is not much contiguous space on the surface left for complete (7×7) unit cells. Therefore due to the limited correlation length the LEED pattern may vanish before the complete surface is converted to a (3×1) reconstruction. Finally, we report that the (3×1) LEED pattern was observed up to Li coverages over 0.5 ML.[16]

The UHV chamber was connected via a differential pumping section to the chamber in which the source for a thermal nuclear spin polarized ^{8}Li atomic beam was installed. Radioactive ^{8}Li with a half life of only 0.84 s was produced *in situ* by bombarding a deuterium gas target with a 24 MeV $^7Li^{3+}$ ion beam from the MP-tandem accelerator at the MPI for Nuclear Physics in Heidelberg inducing the ^{2}H(^{7}Li,^{8}Li)^{1}H nuclear reaction. Its nuclear spin ($I=2$) was polarized by optical pumping in a magnetic field either in the $m=+2$ or in the $m=-2$ state (positive and negative polarization). The source provided at the site of the sample a thermal atomic beam of about 10^8 lithium atoms/s containing a small amount of about 5×10^4 atoms/s of the nuclear spin polarized radioactive isotope ^{8}Li.[32] Only these ^{8}Li atoms served as probes for the measurements of T_1 times (nuclear spin relaxation rates $\alpha=1/T_1$).

^{8}Li is a β-decaying nucleus. Therefore its nuclear polarization (magnetization) can be detected using the β-decay asymmetry.[28] There are more electrons emitted opposite to the direction of the nuclear spin than in its direction. These asymmetries ε were measured with two scintillator telescopes positioned at 0° and 180° in respect to the external magnetic field (see Fig. 1). The asymmetry ε and thus the polarization P of he nuclear spin of the adsorbed ^{8}Li is determined from the normalized difference of the two count rates

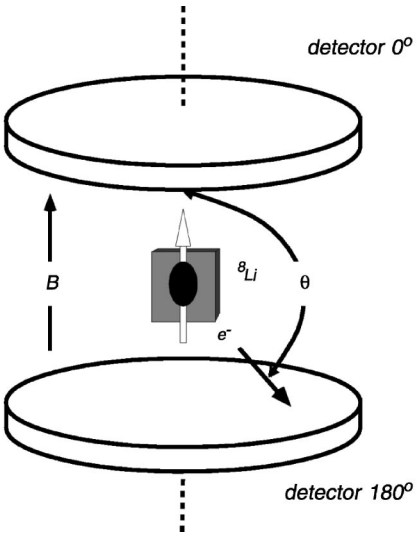

FIG. 1. The principle of β-NMR: The decay electrons are emitted with a higher probability opposite to the direction of the nuclear spin. Therefore, the normalized asymmetry ε of the count rate $N(0°)$ and $N(180°)$ yields the polarization of the spin ensemble.

$$\varepsilon = \frac{N(0°) - N(180°)}{N(0°) + N(180°)} = -\frac{1}{3}P. \tag{1}$$

Here $N(0°)$ and $N(180°)$ denote the count rates of the emitted electrons at the angle indicated. The factor $(-1/3)$ reflects the properties of the ^{8}Li β decay (allowed Gamow-Teller decay, Ref. 39, Vol. 2). Systematic errors in the measurement of the asymmetry are removed by performing measurements with both positive and negative polarizations.

Since ^{8}Li possesses a nuclear spin $I=2$ the decay of nuclear polarization with time (nuclear spin relaxation) can be expressed in general as the sum of four exponentials (for details see Ref. 40 and Appendix A of Ref. 41). In practice, at most two exponentials, fast and slow nuclear spin polarization, were sufficient to describe such data in the past (see detailed discussion in Ref. 33). But it was not always possible to disentangle them with high precision. However, the lowest relaxation rate (smallest depolarization) could always be determined accurately (see Fig. 2, left). We therefore concentrate in this paper on $\alpha_{\text{slow}} \hat{=} \alpha = 1/T_1$ only in describing $\varepsilon(t)$

$$\varepsilon(t) = \varepsilon_0 e^{-\alpha t} = \varepsilon_0 e^{-t/T_1} \tag{2}$$

and postpone the discussion of the other variables, including the determination of ε_0, to a forthcoming publication.

In Fig. 2 two examples of measured asymmetries ε versus time are shown together with fits of the data to Eq. (2). On the left side data at $T=284$ K and $B=0.8$ T are displayed for a Si(111)-(3×1)-Li surface with an additional Li coverage of about 0.14 ML to the 1/3 ML necessary for the formation of the (3×1) reconstruction. A relaxation rate of $\alpha = (0.23 \pm 0.01)\ \text{s}^{-1}$ was obtained by the fit (solid line). On the right side of Fig. 2 data from the Si(111)-(3×1)-Li surface alone at $T=100$ K and $B=0.8$ T are shown (Li coverage in between 10^{-4} and 10^{-2} of a ML). The data show that within the error bars no nuclear spin depolarization occurs and thus the relaxation rate from the fit [$\alpha = (0.007 \pm 0.017)\ \text{s}^{-1}$, solid line] is within the error bars zero.

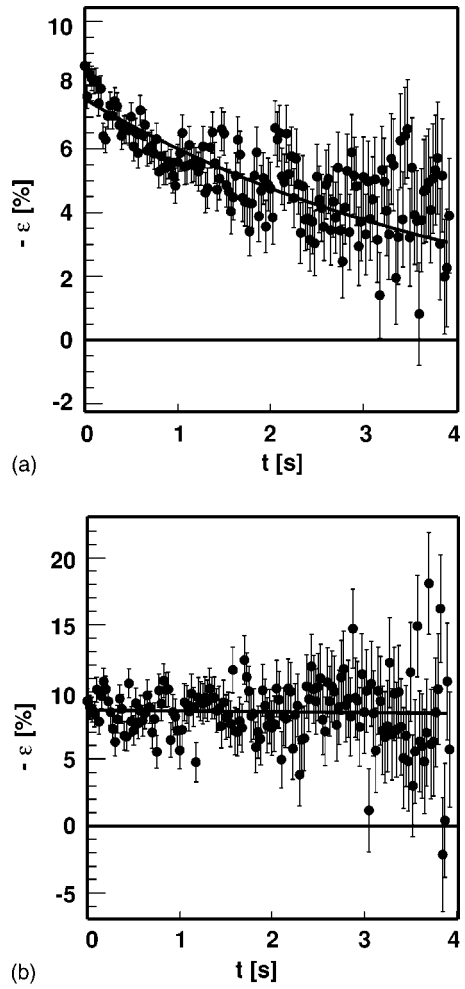

FIG. 2. (a) Asymmetry ε vs time at 284 K for ^{8}Li adsorbed on a Si(111)-(3×1)-Li surface with $\theta_{\text{Li}}=0.47$ ML, that is an Li coverage of about 0.14 ML in addition to the one (1/3 ML) to form the (3×1) reconstruction. (b) Asymmetry ε vs time at 100 K for extremely low Li coverage on a Si(111)-(3×1)-Li surface. No depolarization of the nuclear spin is observed. Both data are measured with a magnetic field of 0.8 T.

We close this section with the remark that contrary to conventional NMR experiments[28–30] the determination of α or T_1 does not require the application of resonant rf fields. Since the nuclear spin polarization P is in thermal equilibrium of the order of 10^{-5}, it can be neglected compared to the initial polarization of the ^{8}Li ensemble of 0.8 or 0.9 (see Ref. 28).

III. EXPERIMENTAL RESULTS

Figures 3–5 display the observed relaxation rates as function of surface temperature, magnetic field and Li coverage θ_{Li}. The data exhibit a rich variation in particular as functions of temperature and coverage. Since for increasing coverage

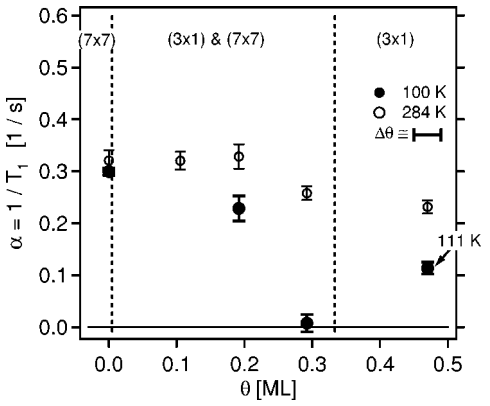

FIG. 3. Nuclear spin relaxation rates $\alpha=1/T_1$ as a function of the Li coverage θ_{Li} of Si(111) surfaces. The data were taken at a magnetic field of $B=0.8$ T. Data taken at temperatures of 100 and 284 K are shown. The lower data point at $\theta_{\mathrm{Li}}\simeq 0.47$ ML (full circle) was taken at 111 instead of 100 K because of experimental reasons.

up to $\theta_{\mathrm{Li}}=1/3$ ML the (3×1) reconstructed islands grow to finally cover the surface totally one would naively expect a continuously decreasing relaxation rate indicating the continuous transition of the surface from a metallic (7×7) to a semiconducting (3×1) one. The data for a surface temperature of 100 K indicate this trend (full circles in Fig. 3). At $\theta_{\mathrm{Li}}\simeq 0.29$ ML, where the entire surface is (3×1) reconstructed, a vanishing relaxation rate is observed (compare also with the lower part of Fig. 2). The temperature dependence of the relaxation rate at this coverage exhibits, however, a kind of thermal activated behavior (Fig. 4). Thus, the coverage dependence of the relaxation rates at an elevated temperature of 284 K appears quite different with respect to what was observed at the lower temperature of 100 K (open circles in Fig. 3). At 100 K the relaxation rate increases again at $\theta_{\mathrm{Li}}\simeq 0.47$ ML, 0.14 ML above the one necessary to complete the semiconducting (3×1) reconstruction. Also, quite surprising temperature dependencies were obtained for this coverage. The data of Fig. 5(a) indicate up to 300 K a linear dependence of the relaxation rate with temperature, which points to a metallic behavior[28,29] (Korringa relaxation). The inset of this figure shows the same data with an additional data point at $T=439$ K with a large error due to a low count rate and a small asymmetry effect ε. Beyond 300 K the relaxation rate seems to rise in addition exponentially (thermally activated). This exponential rise points to diffusion as an additional relaxation mechanism which is supported by the $1/B^2$ magnetic field dependence of the relaxation rates in Fig. 5(b) measured at $T=284$ K. This is a strong indication for such a mechanism (see Sec. IV).

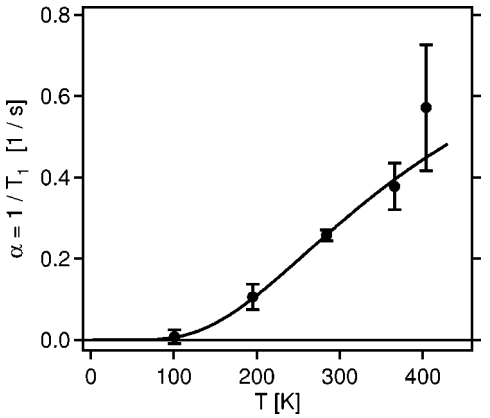

FIG. 4. Nuclear spin relaxation rates $\alpha=1/T_1$ as a function of temperature for ^{8}Li adsorbed on the Si(111)-(3×1)-Li surface at a coverage of $\theta_{\mathrm{Li}}\simeq 0.29$ ML [i.e., the coverage where the entire surface is $(3\times1$ reconstructed]. The data were taken at a magnetic field of $B=0.8$ T. The solid line is a fit to the data (see Sec. IV).

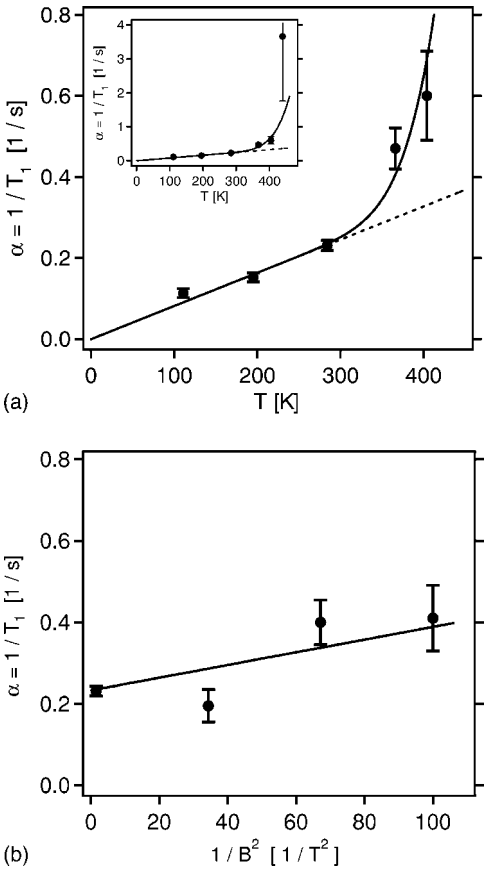

FIG. 5. Nuclear spin relaxation rates $\alpha=1/T_1$ for ^{8}Li adsorbed on the Si(111)-(3×1)-Li surface at a coverage of $\theta_{\mathrm{Li}}\simeq 0.47$ ML [i.e., a fully reconstructed (3×1) surface with an additional coverage of 0.14 ML]. (a) Relaxation rate α as a function of temperature for $B=0.8$ T. The inset shows the data with an additional data point at $T=439$ K which has, however, a very large error bar. (b) Relaxation rate α as a function of $1/B^2$ (the inverse of the magnetic field squared) at $T=284$ K.

IV. DISCUSSION

A. Nuclear spin relaxation on the semiconducting (3×1) surface

For coverages below $\theta_{\mathrm{Li}}=1/3$ ML the as prepared Si(111)-(7×7) surface is developing with increasing coverage larger and larger (3×1) reconstructed islands until the complete reconstruction is reached at $\theta_{\mathrm{Li}}=1/3$ ML. In order

to obtain a systematic understanding of the complex coverage and temperature dependence seen in Figs. 3–5 we start with the discussion of the coverage dependence of the relaxation rates at 100 K, the lowest temperature at which data were taken (full circles in Fig. 3). Up to $\theta_{\mathrm{Li}} = 0.29 \pm 0.02$ ML they meet our expectation. The nuclear spin relaxation rate α starts at very low coverage with the value known for the "metallic" (7×7) reconstruction. At the fully developed semiconducting (3×1) reconstruction it approaches a value consistent with zero. At the coverage in between a value "in between" is adopted reflecting the ratio of the (3×1) reconstructed islands to the remaining (7×7) reconstructed surface. The increasing relaxation rate beyond $\theta_{\mathrm{Li}} = 1/3$ ML will be discussed in the next subchapter.

Prior to a discussion of the coverage dependence at the elevated temperature (open circles in Fig. 3) we discuss first the temperature dependence of the relaxation rates at $\theta_{\mathrm{Li}} \simeq 0.29$ ML at which already a complete (3×1) reconstructed and thus semiconducting surface was observed (Fig. 4). The relaxation rates seem to vanish below 100 K and their temperature dependence points to a kind of thermal activated process. At first glance diffusive relaxation as the underlying mechanism comes into one's mind, as, e.g., observed for Li adsorption on a Ru(001) surface[41,42] or here at a coverage of $\theta_{\mathrm{Li}} \simeq 0.47$ ML (see next subsection). Using thermal activated diffusion in a BPP model,[28,29] named after the initials of its authors,[43] the data of Fig. 4 can indeed be perfectly described with the aid of Eqs. (7) and (8). (The result of the fit is almost not distinguishable from the solid line in Fig. 4.) However, the extremely small diffusion energy of $E_{\mathrm{diff}} = 48 \pm 10$ meV and the extremely large prefactor of $\tau_0 = (5 \pm 2) \times 10^{-7}$ s found renders this model very unlikely to describe the real origin of the fluctuations causing the relaxation rates of Fig. 4. (With the "standard" prefactor of $\tau_0 = 10^{-13}$ s, Ref. 44, it was not possible to describe the data at all.) Consequently, we have to envisage electronic relaxation (fluctuating electron spins) as the most probable origin of the observed relaxation rates.

The main source of electronic nuclear spin relaxation is caused by Fermi contact interaction of the nuclear spin with fluctuating electron spins.[28,29] Since for all realistic situations the electron correlation time is much smaller than the nuclear Larmor period (at $B = 0.8$ T, for ^{8}Li, $1/\nu_L \simeq 0.2$ μs), the relaxation rate for a electronic relaxation mechanism is independent of the magnetic field strength. For nuclear spin relaxation (depolarization) to occur the necessary energy change for the mutual spin flip of the nucleus and the electron can happen only for electrons which occupy states with energies for which occupied and unoccupied states exist. These are for a degenerate electronic system the ones near the Fermi energy. Then the relaxation rate becomes strictly linear in temperature as observed, e.g., on metal surfaces[41,45] [see also Fig. 5(a)]. But this approach does not allow a vanishing relaxation rate for $T > 0$ K as observed on the completely (3×1) reconstructed surface (Fig. 4). As this surface is definitely semiconducting the description of the relaxation process has to be adopted to this situation.

On a semiconducting surface there are no electrons at the Fermi energy. Thus, Fermi contact interaction of nuclear spins with electron spins is only possible with electrons in the conduction band. As the band gap of the (3×1) reconstructed surface is quite large (about 1 eV[11]) nuclear spin relaxation with intrinsic electrons would not be observable below temperatures of about 500 K. Therefore we are forced to consider another mechanism for semiconducting surfaces: Li atoms themselves adsorbing during the nuclear spin relaxation measurements or here also small quantities of surplus Li from the formation of the (3×1) reconstruction may act as dopants of the surface. Electrons from a donor level are excited into the conduction band at low temperatures and thus, nuclear spin relaxation due to Fermi contact interaction may be observable also at lower temperatures. For bulk semiconductors such a situation leads to a $\sqrt{T}$ dependence of the relaxation rates[29] which is certainly not in agreement with the observed temperature dependence of the relaxation rate α in Fig. 4. In order to see whether the lower dimensionality of our problem is the reason for the kind of thermal activated temperature dependence found here, we reformulated for a two-dimensional system the theoretical treatment originally formulated for bulk semiconductors assuming that the Li dopants are concentrated in a two-dimensional layer on the surface.

Thus, the electron gas in the conduction band will be delocalized in two dimensions only and localized in the third one perpendicular to the surface, say for simplicity within an infinite high rectangular potential barrier of width L. Aside from this assumption we will follow the conventional treatment of relaxation rates and electron densities in the valence band, in particular we will treat the electrons as nondegenerate with a Boltzmann distribution. The essential steps to find the final result

$$\alpha = \frac{1}{T_1} = \frac{2\pi}{\hbar}\frac{32\pi^2}{9}\mu_e^2\left(\frac{\mu_I}{I}\right)^2 \cdot |\Phi(0)|^4 \cdot \rho^{(2)} \cdot n^{(2)}(T) \quad (3)$$

can be found in the Appendix, whereas μ_e and μ_I denote the magnetic moments of the electron and the nucleus, respectively. $|\Phi(0)|^2$ is the (energy independent) probability to find an electron at the nucleus (and thus a dimensionless number) and $\rho^{(2)}$ the energy independent density of states per volume of a two-dimensional free electron gas which is localized in the third dimension perpendicular to the surface within a rectangular potential barrier of width L,[46]

$$\rho^{(2)} = \frac{1}{L\pi} \cdot \frac{m^*}{\hbar^2}, \quad (4)$$

where m^* denotes the effective electron mass in the conduction band. (Contrary to the original work of Abragam[29] $\rho^{(2)}$ denotes the total density of states rather the one for a specific electronic spin state.) The only temperature dependent factor in Eq. (3) is the two-dimensional electron density $n^{(2)}(T)$ in the conduction band for a nondegenerate electron gas (analogous formula as in three dimensions, see, e.g., Ref. 46)

$$n^{(2)}(T) = \frac{2n_D^{(2)}}{1 + \sqrt{1 + 4\dfrac{n_D^{(2)}}{n_0^{(2)}(T)} \exp\left(\dfrac{E_D}{kT}\right)}}. \quad (5)$$

The factor $n_D^{(2)}$ is the area density of the donors and $n_0^{(2)}(T)$ a suitable normalization factor for the two-dimensional problem

$$n_0^{(2)}(T) = \frac{1}{L}\frac{m^*}{\pi\hbar^2}kT. \quad (6)$$

E_D in Eq. (5) denotes the energy difference between the donor level and the conduction band.

From Eq. (5) it is obvious that for small enough donor densities $n_D^{(2)}$ [i.e., $n_D^{(2)} \ll n_0^{(2)}(T)$] or high enough temperatures the electron density in the conduction band $n^{(2)}(T)$ would equal the donor density $n_D^{(2)}$ and thus $n^{(2)}(T)$ becomes temperature independent. Consequently, the relaxation rate α would become temperature independent as well. But contrary to the three-dimensional problem in two dimensions (i.e., on a surface) high donor densities in respect of $n_0^{(2)}(T)$ are possible. There are about 2×10^{15} adsorption sites on a Si(111) single crystal surface and thus the coverage dependent donor density amounts to $n_D^{(2)} = (2\times10^{15}\ \theta_{\mathrm{Li}})/(L\ \mathrm{cm}^2)$. At a temperature of 300 K $n_0^{(2)}(T)$ [Eq. (6)] has a value of about $10^{13}/(L\ \mathrm{cm}^2)$ and thus the ratio $n_D^{(2)}/n_0^{(2)}(T)$ in Eq. (5) amounts to about $2\times10^2\ \theta_{\mathrm{Li}}$ at 300 K. Under these circumstances the nuclear spin relaxation process described above would show a pronounced temperature dependence even for θ_{Li} as low as 10^{-2}–10^{-4} ML [Eqs. (3) and (5)].

The solid line in Fig. 4 shows a fit to the data based on the relaxation process described above [Eqs. (3)–(5)]. For the measurements without any additional coverage the Li dose stems either from adsorbed Li out of the atomic beam during data taking or from surplus Li from the preparation of the (3×1) reconstruction. Thus, the Li coverage is known to be small, but not exactly how small. Furthermore, because of the unknown width L of the two-dimensional surface layer the temperature independent prefactors in Eq. (3), in particular $|\Phi(0)|^2$, cannot be determined. Therefore Fig. 6 shows fits to the data for three coverages, each differing by one order of magnitude. Obviously it is possible to fit the data in Fig. 6 with all coverages assumed yielding values for E_D which vary only in between 80 and 120 meV (see Table I). Accordingly, however, the ratio $|\Phi(0)|^2/L$ changes by about one order of magnitude to compensate for the different values of θ_{Li}. The values found for E_D are larger than the one known for Li doping of Si single crystals (about 32 meV, Refs. 47–49). The insensitivity of the results in the low coverage regime (Fig. 6) also solves another puzzle. Due to accumulated ^{8}Li and in particular ^{7}Li atoms from the atomic beam, the actual Li coverage on the surface is rising during the runs which sometimes last for about 2 h before a fresh surface is prepared. Nevertheless, the measured relaxation rates α were found to be time and thus coverage independent in the temperature regime investigated.

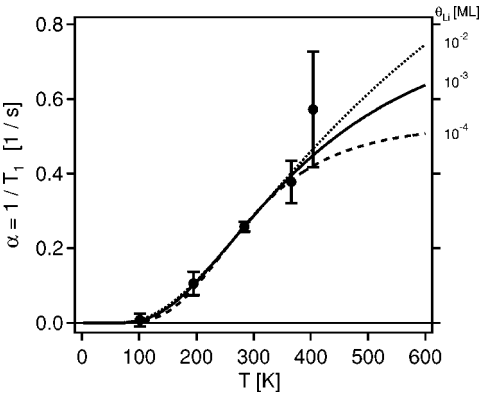

FIG. 6. Nuclear spin relaxation rates $\alpha = 1/T_1$ as a function of temperature for ^{8}Li adsorbed on the Si(111)-(3×1)-Li surface at a coverage of $\theta_{\mathrm{Li}} \simeq 0.29$ ML (same data as Fig. 4). Fits of the relaxation model on semiconductor surfaces with three different Li coverages θ_{Li} are shown.

Having this interpretation in mind we can now also understand the coverage dependence at 284 K (open circles in Fig. 3). First the data point at $\theta_{\mathrm{Li}} \simeq 0.29$ ML is just part of the ones in Figs. 4 resp. 6 and its value follows from the arguments given above. It deviates from zero as observed for 100 K because thermal activated Li donor atoms contribute to electronic relaxation. At lower coverages the relaxation rates seem to be enhanced as compared to the low temperature data (Fig. 3). That is probably of the same origin: on the (3×1) reconstructed islands adsorbed Li acts as donor and contributes together with the relaxation from the remaining metallic (7×7) reconstructed parts additionally to the relaxation rate α.

B. Adsorption of additional Li on the (3×1) reconstructed surface

At a Li coverage of $\theta_{\mathrm{Li}} \simeq 0.47$ ML that is an additional 0.14 ML aside from the 1/3 ML necessary to generate the Si(111)-(3×1)-Li surface the nuclear spin relaxation rates α are considerably different from those found for a coverage of $\theta_{\mathrm{Li}} \simeq 0.29$ ML [see Figs. 4 and 5(a)]. The first three data points are in accordance with a straight line crossing the abscissa at zero [dashed line in Fig. 5(a)]. This points to a metallic system ("Korringa" relaxation, Ref. 28, 29, 41, 45, and 50). As the (3×1) reconstruction is formed at a coverage of $\theta_{\mathrm{Li}} = 1/3$ ML the surface with a coverage of $\theta_{\mathrm{Li}} \simeq 0.47$ ML may be considered for the time being as an inert semiconducting surface with an additional Li coverage of $\theta_{\mathrm{Li,add}} \simeq 0.14$ ML.

There are at least two possible ways that a semiconducting surface can be transformed into a metallic one by adsorb-

TABLE I. Energy difference E_D between the donor level and the conduction band for different Li coverages θ_{Li}.

θ_{Li} (ML)	10^{-2}	10^{-3}	10^{-4}
E_D (meV)	80±18	92±17	116±16

ing an alkali-metal such as Li. First, the growing density of the adsorbate can induce an overlap of the wave functions of the valence electrons (2s for Li) and thus lead to delocalization (Mott criterion[51–53]). Second, the electrons injected into the system by the Li adsorbate can fill an unoccupied surface state near the Fermi-energy E_F. In this case E_F would be pinned at this state and the surface would be metallic. This possibility was, for example, favored to describe on the semiconducting Si(001) surface an additional surface state at E_F during Li adsorption ($\theta_{\mathrm{Li}} \approx 0.08 \ldots 0.36$ ML).[54]

The first possibility is rather unlikely to occur here as the nuclear spin relaxation rates, e.g., on the semiconducting Si(111)-(1×1):H surface covered with 0.25 ML Li can still be described assuming a semiconducting surface.[55] Thus, the second possibility seems to be the more realistic one. And indeed the calculated band structure based on the HCC model[13] of the Si(111)-(3×1) surface predicts an unoccupied surface state near E_F (called S_1^- in Ref. 13) while on the Si(111)-(1×1):H surface there exists no surface state in the fundamental band gap at all.[2,56]

At temperatures above about 300 K the nuclear spin relaxation rates start to deviate from the straight line [Fig. 5(a)]. It looks as to whether an additional probably thermal activated relaxation process starts to become active. And indeed, relying on results of previous experiments it may be identified with relaxation induced by the diffusion of the Li atoms over the surface. The mechanism was explained in large detail in a former paper for a metallic Ru(001) surface.[41] Through binding to the surface an electric dipole moment is induced at the Li atom. That is also true at semiconducting surfaces at least for small coverages. The Li atoms generate therefore an electric field gradient (EFG) around them (electric field of a dipole $\sim 1/r^3$). Diffusing over the surface from time to time a ^{8}Li atom passes closely enough another Li atom, leading to a fluctuating interaction in time of the quadrupole-moment of the first one with the EFG generated by the second one. This mechanism can be the cause of thermal activated diffusive relaxation.

The nuclear spin relaxation rates α_{diff} induced by diffusion can phenomenologically be described with the BPP model[28,29,43]

$$\alpha_{\mathrm{diff}} = \frac{G(0)}{\hbar^2} \frac{2\tau_c}{1 + (\omega_L \tau_c)^2}. \tag{7}$$

The factor $G(0)$ characterizes the strength of the fluctuating interaction, ω_L is the Larmor frequency which is proportional to the external magnetic field B. The correlation time τ_c can be interpreted as the mean residence time of the ensemble on an adsorption site and can be expressed in terms of a prefactor τ_0 and the diffusion barrier E_{diff}

$$\tau_c = \tau_0 \exp\left(\frac{E_{\mathrm{diff}}}{kT}\right). \tag{8}$$

For $\omega_L \tau_c \gg 1$ (i.e., for low enough temperatures) the relaxation rate should show a $1/B^2$ dependency [see Eq. (7)] in accordance with the results of the magnetic field dependence observed for $\alpha = 1/T_1$ [Fig. 5(b)]. This supports the assumption of an additional relaxation mechanism with correlation times $\tau_c \gg 1/\omega_L$ to be valid. We remind here that for electronic relaxation always $\tau_c \ll 1/\omega_L$ which is the reason that it does not contribute to the magnetic field dependence of α.

The solid curves in Figs. 5(a) and 5(b) show a fit based on electronic Korringa relaxation α_{Korr}, linear in temperature, plus relaxation by diffusion:

$$\alpha = \alpha_{\mathrm{Korr}} + \alpha_{\mathrm{diff}}. \tag{9}$$

There are in general four parameters to be adjusted: $G(0)$, τ_0, E_{diff} and the slope of the straight line $(T_1T)_{\mathrm{Korr}}$. But since in the temperature regime investigated $\omega_L \tau_c \gg 1$ only the ratio $G(0)/\tau_0$ can be determined by the fit. If for $G(0)$ a typical value of $(10^{-11}\ \mathrm{eV})^2$ is assumed (see Refs. 41 and 57) one obtains with a large error the prefactor $\tau_0 \approx 10^{-12}$ s in agreement with the typical value around 10^{-13} s (Ref. 44). The other two parameters E_{diff} and $(T_1T)_{\mathrm{Korr}}$ depend only weakly on variations of $G(0)/\tau_0$.

For the diffusion barrier a value of $E_{\mathrm{diff}} \approx 410$ meV is obtained by the fit. At an external magnetic field of $B = 0.8$ T and at a temperature of 300 K this leads to a value for $\omega_L \tau_c = 244$ (for $\tau_0 = 10^{-12}$ s) confirming the assumption of $\omega_L \tau_c \gg 1$. The value for E_{diff} is significantly smaller than the ones found for diffusion of alkali metals and H on Si(111) surfaces: Li about 1 eV, Ref. 57; H about 1.7 to 2 eV, Ref. 58; K, Rb and Cs about 1.6–1.9 eV, Ref. 59. This difference can most likely be explained by the different surface reconstructions used in the diffusion experiments, high temperature (1×1) phase in Ref. 57 and the (7×7) reconstruction in Refs. 58 and 59. For the electronically driven part of the nuclear spin relaxation a value of $(T_1T)_{\mathrm{Korr}} = 1220 \pm 50$ s K is found [dashed line in Fig. 5(a)]. This value is significantly higher than the value of $(T_1T)_{\mathrm{Korr}} = 498 \pm 117$ s K found on the metallic (7×7) reconstructed surface at lower magnetic fields.[33]

V. SUMMARY

Li adsorption on the (3×1)-Li reconstructed Si(111) surface has been studied in nuclear spin relaxation (NMR) experiments with the probe ^{8}Li. A rich variety of temperature, coverage and magnetic field dependencies were observed, which reflect a metal-semiconductor-metal transition while adsorbing Li with increasing coverage on a (7×7)-reconstructed Si(111) surface in such a way that the (3×1) reconstruction is driven. At a Li coverage of $\theta_{\mathrm{Li}} = 0.29 \pm 0.02$ ML, just the one for a perfect (3×1) reconstruction to occur ($\theta_{\mathrm{Li}} = 1/3$ ML), the observed relaxation rates can be explained by an electronically driven process on a semiconducting surface with a two-dimensional Li induced donor level about 100 meV below the conduction band.

At a higher coverage of $\theta_{\mathrm{Li}} \approx 0.47$ ML a Korringa-like relaxation behavior is observed which points surprisingly to a metallic surface at a coverage of only 0.14 ML beyond the 1/3 ML to form the (3×1) reconstruction. The difference to Li adsorption on the semiconducting Si(111)-(1×1):H surface which stays semiconducting even for higher coverages[55] can be explained by the fact that there are no surface states within the fundamental band gap of the latter,[2,56] while for

the Li induced (3×1) reconstruction at least theoretically an empty state (called S_1^-) is predicted near the Fermi energy. Li valence electrons may fill this state pinning the Fermi energy and causing in this way the metallicity of the surface at quite low additional Li coverage. Unfortunately, this filled surface state is not observed yet in photoemission experiments probably due to selection rules and an improper polarization of the used synchrotron light. Using the proper polarization of the synchrotron light it would, however, be very interesting to compare our results with photoemission data from the (3×1) reconstruction with additional alkali-metal coverage. At temperatures above 284 K an additional relaxation process caused by diffusion of the Li atoms over the surface with a diffusion barrier of about 410 meV is found. This value is significantly smaller than the ones found for diffusion of alkalis and H on other Si(111) surfaces.

In summary, out of this experiment a consistent picture of the temperature, coverage and magnetic field dependence of T_1 times emerged. With the aid of a formulated concept of Li donors localized on a semiconducting surface the temperature dependence of relaxation rates for Li adsorbed on the (3×1) reconstructed Si(111) surface could be understood consistently. As a by-product the donor energy of adsorbed Li on the (3×1) surface could be determined. This success proves additionally that the theoretical results of a completely ionized Li chain in the (3×1)-reconstruction is correct. If not, the remaining electrons at the Li chains and consequently the missing ones at the Si atoms forcing the (3×1) reconstruction would be able to fluctuate and thus contribute to the relaxation rate. Since, in contrast to Li adsorption on the (7×7) surface,[60,61] this mechanism is missing electron-electron correlations probably affect the energy of surface states only but not T_1 times. The observed semiconductor-metal transition for adsorption of 0.14 ML additional Li on the already (3×1)-reconstructed surface points to the existence of an empty state near the Fermi-energy (probably the so-called S_1^- state). Here as a by-product an estimate for the diffusion energy of Li on the Si(111)-(3×1) surface could be obtained as well.

ACKNOWLEDGMENTS

This work was supported by the Deutsche Forschungsgemeinschaft (DFG), Bonn. We acknowledge the invaluable support of the Max-Planck-Institut für Kernphysik, Heidelberg, at which the experiments were performed.

APPENDIX

In order to derive an expression for the relaxation rate of a nuclear spin in a two-dimensional nondegenerate electron gas we start with Eq. (58) of Chapter IX in Abragam's textbook *Principles of Nuclear Magnetism*[29]

$$\frac{1}{2T_1}=\frac{2\pi}{\hbar}\left(\frac{8\pi}{3}\gamma_e\gamma_n\hbar^2\right)^2\frac{1}{4}|\Phi(0)|^4\int_0^\infty P(E)\rho^2(E)dE, \tag{A1}$$

where $\rho(E)$ is the density of states for a three-dimensional electron gas for a given spin orientation, $|\Phi(0)|^2$ the (energy independent) probability to find an electron at the nucleus (a dimensionless quantity) and $P(E)=a\cdot\exp(-E/kT)$. The integral runs from the bottom of the conduction band to infinity. The constant a and thus implicitly the Fermi energy is determined by requiring the normalization

$$\int_0^\infty \rho(E)P(E)dE=a\int_0^\infty \rho(E)e^{-E/kT}dE=\frac{1}{2}n(T). \tag{A2}$$

The factor $1/2$ appears, since $\rho(E)$ is chosen in Abragam's treatment to be the density of states for only one spin orientation.

To deal with a two-dimensional electron gas being bound within a (infinite high) potential well of width L in the third direction (surface normal) we have to replace ρ by $\rho^{(2)}/2$ of Eq. (4) ($\rho^{(2)}$ is the density of states including both spin directions) and $n(T)$ by $n^{(2)}(T)$ of Eq. (5). Having in mind that the gyromagnetic ratio of a particle with spin I is related to its magnetic moment by $\gamma=\mu/\hbar I$ and that the spin of the electron is $1/2$, one obtains Eq. (3) straightaway.

For the derivation of $n^{(2)}(T)$ the dimensionality of the problem matters only in so far that the now energy independent two-dimensional density of states always has to be used [Eq. (4)]. Otherwise, as usual, only the approximation that the electrons in the conduction band are not degenerate (Boltzmann distributed) enters.[46,62] Furthermore, we assumed that we are dealing with temperatures where thermal intrinsic activation out of the valence band can be neglected and only the thermal activated donor electrons contribute to the conduction band.

[1] R. Losio, K. N. Altmann, and F. J. Himpsel, Phys. Rev. B **61**, 10845 (2000).
[2] J. J. Paggel, W. Mannstadt, C. Weindel, M. Hasselblatt, K. Horn, and D. Fick, Phys. Rev. B **69**, 035310 (2004).
[3] C. Bromberger, J. N. Crain, K. N. Altmann, J. J. Paggel, F. J. Himpsel, and D. Fick, Phys. Rev. B **68**, 075320 (2003).
[4] B. N. J. Persson and J. E. Demuth, Phys. Rev. B **30**, 5968 (1984).
[5] F. J. Himpsel, G. Hollinger, and R. A. Pollack, Phys. Rev. B **28**, 7014 (1983).
[6] F. J. Himpsel and T. Fauster, J. Vac. Sci. Technol. A **2**, 815 (1984).
[7] E. Louis, F. Flores, F. Guinea, and C. Tejedor, Solid State Commun. **44**, 1633 (1982).
[8] X. Blase, X. Zhu, and S. G. Louie, Phys. Rev. B **49**, 4973 (1994).
[9] J. Ortega, F. Flores, and A. L. Yeyati, Phys. Rev. B **58**, 4584 (1998).
[10] M. Tikhov, L. Surnev, and M. Kiskinova, Phys. Rev. B **44**, 3222 (1991).
[11] D. Jeon, T. Hashizume, T. Sakurai, and R. F. Willis, Phys. Rev. Lett. **69**, 1419 (1992).

[12] H. H. Weitering, X. Shi, and S. C. Erwin, Phys. Rev. B **54**, 10585 (1996).
[13] S. C. Erwin and H. H. Weitering, Phys. Rev. Lett. **81**, 2296 (1998).
[14] H. Daimon and S. Ino, Surf. Sci. **164**, 320 (1985).
[15] E. Bauer and H. Poppa, Thin Solid Films **12**, 167 (1972).
[16] H. Kleine, H. Bludau, H. Over, and D. Fick, Surf. Sci. **410**, 15 (1998).
[17] J. J. Paggel, G. Neuhold, H. Haak, and K. Horn, Phys. Rev. B **52**, 5813 (1995).
[18] S. Hasegawa, M. Maruyama, Y. Hirata, D. Abe, and H. Nakashima, Surf. Sci. **405**, L503 (1998).
[19] L. Lottermoser, E. Landemark, D.-M. Smilgies, M. Nielsen, R. Feidenhans'l, G. Falkenberg, R. L. Johnson, M. Gierer, A. P. Seitsonen, and H. Kleine *et al.*, Phys. Rev. Lett. **80**, 3980 (1998).
[20] C. Collazo-Davila, D. Grozea, and L. D. Marks, Phys. Rev. Lett. **80**, 1678 (1998).
[21] M.-H. Kang, J.-H. Kang, and S. Jeong, Phys. Rev. B **58**, R13359 (1998).
[22] A. A. Saranin, A. V. Zotov, V. G. Lifshits, M. Katayama, and K. Oura, Surf. Sci. **426**, 298 (1999).
[23] A. A. Saranin, A. V. Zotov, V. G. Lifshits, J.-T. Ryu, O. Kubo, H. Tani, T. Harada, M. Katayama, and K. Oura, Phys. Rev. B **58**, 3545 (1998).
[24] H. Kleine and D. Fick, New J. Phys. **3**, 1.1 (2001).
[25] T. Okuda, H. Ashima, H. Takeda, K.-S. An, A. Harasawa, and T. Kinoshita, Phys. Rev. B **64**, 165312 (2001).
[26] M. Gurnett, J. B. Gustafsson, K. O. Magnusson, S. M. Widstrand, and L. S. O. Johansson, Phys. Rev. B **66**, 161101 (2002).
[27] S. Jeong and M.-H. Kang, Phys. Rev. B **54**, 8196 (1996).
[28] G. Schatz and A. Weidinger, *Nuclear Condensed Matter Physics* (Wiley, Chichester, 1996).
[29] A. Abragam, *Principles of Nuclear Magnetism* (University Press, Oxford, 1978).
[30] C. P. Slichter, *Principles of Magnetic Resonance* (Springer, Berlin, 1992).
[31] D. Fick, R. Veith, H. D. Ebinger, H. J. Jänsch, C. Weindel, H. Winnefeld, and J. J. Paggel, Phys. Rev. B **60**, 8783 (1999).
[32] H. J. Jänsch, G. Kirchner, O. Kühlert, M. Lisowski, J. J. Paggel, R. Platzer, R. Schillinger, H. Tilsner, C. Weindel, and H. Winnefeld *et al.*, Nucl. Instrum. Methods Phys. Res. B **171**, 537 (2000).
[33] H. Winnefeld, M. Czanta, G. Fahsold, H. J. Jänsch, G. Kirchner, W. Mannstadt, J. J. Paggel, R. Platzer, R. Schillinger, and R. Veith *et al.*, Phys. Rev. B **65**, 195319 (2002).
[34] W. Widdra, M. Detje, H. D. Ebinger, H. J. Jänsch, W. Preyß, H. Reich, R. Veith, D. Fick, M. Röckelein, and H.-G. Völk, Rev. Sci. Instrum. **66**, 2465 (1995).
[35] M. Detje, M. Röckelein, W. Preyß, H. D. Ebinger, H. J. Jänsch, H. Reich, R. Veith, W. Widdra, and D. Fick, J. Vac. Sci. Technol. A **13**, 2532 (1995).
[36] G. S. Higashi, Y. J. Chabal, G. W. Trucks, and K. Raghavachari, Appl. Phys. Lett. **56**, 656 (1990).
[37] C. Weindel, H. J. Jänsch, J. J. Paggel, R. Veith, and D. Fick, Surf. Sci. **543**, 29 (2003).
[38] S. Olthoff and M. E. Welland, J. Vac. Sci. Technol. B **14**, 1019 (1996).
[39] S. R. de Groot, H. A. Tolhoek, and W. J. Huiskamp, in *Alpha, Beta and Gamma Ray Spectroscopy*, edited by K. G. Siegbahn (North-Holland, Amsterdam, 1965).
[40] M. Riehl-Chudoba, U. Memmert, and D. Fick, Surf. Sci. **245**, 180 (1991).
[41] H. D. Ebinger, H. Arnolds, C. Polenz, B. Polivka, W. Preyß, R. Veith, D. Fick, and H. J. Jänsch, Surf. Sci. **412/413**, 586 (1998).
[42] H. D. Ebinger, H. J. Jänsch, C. Polenz, B. Polivka, W. Preyß, V. Saier, R. Veith, and D. Fick, Phys. Rev. Lett. **76**, 656 (1996).
[43] N. Bloembergen, E. M. Purcell, and R. V. Pound, Phys. Rev. **73**, 679 (1948).
[44] S. Ovesson, A. Bogicevic, G. Wahnström, and B. I. Lundqvist, Phys. Rev. B **64**, 125423 (2001).
[45] H. J. Jänsch, H. Arnolds, H. D. Ebinger, C. Polenz, B. Polivka, G. J. Pietsch, W. Preyß, V. Saier, R. Veith, and D. Fick, Phys. Rev. Lett. **75**, 120 (1995).
[46] H. Ibach and H. Lüth, *Solid-State Physics* (Springer, Berlin, 2003).
[47] C. S. Fuller and J. A. Ditzenberger, Phys. Rev. **91**, 193 (1953).
[48] G. Feher, Phys. Rev. **114**, 1219 (1959).
[49] R. K. Crouch and T. E. Gilmer, J. Phys. Chem. Solids **30**, 2037 (1969).
[50] W. Mannstadt and G. Grawert, Phys. Rev. B **52**, 5343 (1995).
[51] J. M. Ziman, *Principles of the Theory of Solids* (Cambridge University Press, Cambridge, England, 1964).
[52] O. Madelung, *Introduction to Solid-State Theory* (Springer, Berlin, 1978).
[53] N. F. Mott, *Metal-Insulator Transitions*, 2nd ed. (Taylor & Francis, London, 1990).
[54] K. D. Lee, C. Y. Kim, and J. W. Chung, Surf. Sci. **366**, L709 (1996).
[55] C. Weindel, M. Czanta, H. J. Jänsch, G. Kirchner, J. J. Paggel, H. Winnefeld, and D. Fick (unpublished).
[56] K. Hricovini, R. Günther, P. Thiry, A. Taleb-Ibrahimi, G. Indlekofer, J. E. Bonnet, P. Dumas, Y. Petroff, X. Blase, and X. Zhu *et al.*, Phys. Rev. Lett. **70**, 1992 (1993).
[57] J. Chrost and D. Fick, Surf. Sci. **343**, 157 (1995).
[58] R.-L. Lo, I.-S. Hwang, M.-S. Ho, and T. T. Tsong, Phys. Rev. Lett. **80**, 5584 (1998).
[59] R. Storch, H. Stolz, and H.-W. Wassmuth, Ann. Phys. (Leipzig) **1**, 315 (1992).
[60] D. Fick, Hyperfine Interact. **136/137**, 467 (2001).
[61] R. Schillinger, Ph.D. thesis, Philipps-Universität, Marburg, 2003.
[62] R. G. Chambers, *Electrons in Metals and Semiconductors* (Chapman and Hall, London, 1990).